Stochastic Modelling and Computational Sciences

VARIABLE COUPLING BETWEEN IONOSPHERE AND LOWER ATMOSPHERE DURING HUNGA-TONGA VOLCANIC ERUPTION USING COSMIC-SATELLITE

Dr. Gopal Mondal
Assistant Professor, Department of Mathematics, Vivekananda Mission Mahavidyalaya, Haldia, Purba Medinipur, 721645, India

ABSTRACT
The purpose of this paper is to study the sensible variation in the ionosphere during the great Hunga-Tanga volcanic explosion from December 2021 to January 2022 using COSMIC satellite remote sensing data. This study has been carried out mainly based on daily averaged NmF2, HmF2, BTEC, and TTEC values. All four parameters showed significant irregularities from the preparation phase of volcanic eruptions to the post-eruption phase. Specifically, for the ionospheric E-layer, the phases of Ne concentration are opposite to the F layer, with minimal concentrations of peak Ne and ETEC in the pre-eruption phase and noticeable higher concentrations in the post-eruption phase. The variability in ionospheric parameters clearly indicates the good correlation and coincidence between the ionosphere and lower atmospheric disturbances associated with two volcanic explosions. The wave-induced coupling mechanism is mainly responsible for this good coincidence.

Keywords: Volcanic eruption, Gravity wave, Ionosphere, Lower Atmosphere, Coupling

INTRODUCTION
We know a lot about surface volcanoes, including Mount St. Helens in the US, Mount Fuji in Japan, and Mount Merapi in Indonesia. But we know very little about the hundreds of submarine volcanoes scattered across the globe. The Hunga Tonga-Hunga Ha'apai (HTHH) volcano, located approximately 70 km northwest of Nuku'alofa Island, which is the capital city of Tonga at 20.50S and 175.385W, was a little-known seamount along a chain of 20 similar volcanoes that make up the Tongan part of the Pacific "Ring of Fire. Though almost all volcanoes in Tonga are more or less still active, previous significant eruptions of this volcano occurred in 1912, 1937, 1988, and 2009. During the 2009 violent volcanic eruption, it generated ash and steam that reached as high as approximately 7 km altitude and posed risks to air traffic in the region. Initially, the volcanic unrest triggered on HTHH with unprecedented features, leading to an eruption across December 20th, 2021, which lasted to the end of January 2022. During this period, on January 15th, 2022, the HTHH volcanic explosion showed unique characteristics, which was the only event after the 1883 Krakatau, initiating a volcanic tsunami that created waves in the atmosphere by the dual-mechanism generation process comprising atmospheric pressure waves and eruption-induced water displacements (Heidarzadeh *et al.*, 2022). The major gaseous components in this volcanic eruption were water vapor, carbon dioxide, sulfur dioxide, hydrogen chloride, hydrogen fluoride, and hydrogen sulfide, with minor amounts of radon, helium, hydrogen, and carbon monoxide (Chernogor, 2022).

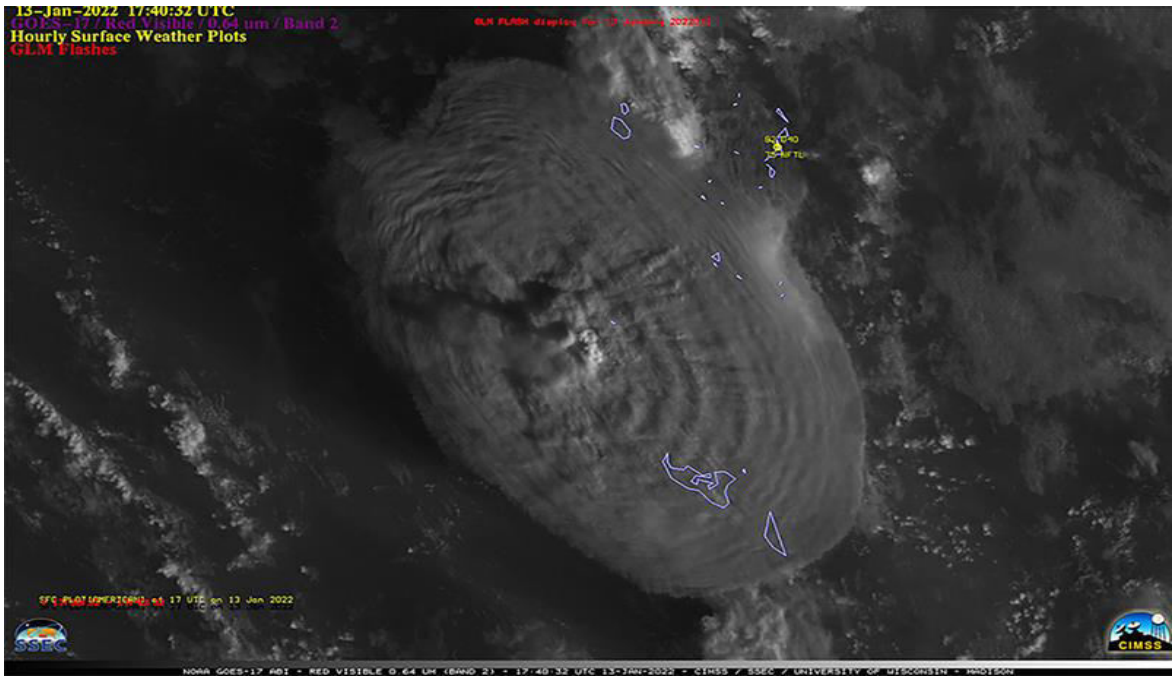

Fig.1: A massive eruption plume rising above HTHH was captured by the GOES-17 satellite at 0640 on 14 January 2022. The plume rose above 16 km altitude and expanded 240-260 km in diameter at the top (Taken from Smithsonian Institution, National Museum of Natural History, Global Volcanism Program; https://volcano.si.edu/volcano.cfm?vn=243040).

Many studies dealings with the HTHH volcanic explosion have been concerned with the impacts of the tsunamis, the effects of the blast waves, the ionospheric hole, the traveling ionospheric disturbances (TID) (Themens *et al.*, 2022), the rearrangement of the ionospheric circuit current system and neutral wind system, and disturbances in the geomagnetic field (Chernogor, 2022). Also, relatively low content of sulfur dioxide in volcanic cocktail of ash, gas, and pulverized rock, researchers are assuming it is the cooling effect (Jenkins *et al.*, 2023) Though initially water vapor radiative cooling and volcanic aerosol cooling dominated the stratospheric cooling and heating rates, after a few days, water vapor heating started to dominate the stratospheric top-of-the-atmosphere radiative forcing, leading to a net warming of the climate system (Sellitto *et al.*, 2022). Another study by Schoeberl *et al.* (2022) reported that the water vapor layer (i.e., the H_2O layer) consistently moves upward with the residual vertical velocity while the descending aerosol layer is gravitationally settling. Even a month after the eruption, a distinct aerosol and water vapor layer formed in the tropical Southern Hemisphere (SH) stratosphere. Thereafter, the water vapor layer is slightly displaced above the aerosol layer near about 26 km altitude, which continued to persist in the tropical SH stratosphere until the end of June while slowly moving apart in altitude. Besl, in his study (Besl, 2023) reported that the HTHH volcanic eruption on 2021–2022, potentially contributing to global warming over the next 5 years, was due to the unprecedented explosion below the ocean surface injecting megatons of vaporized seawater into the stratosphere like a syringe. In Matoza *et al.* 2022, it was reported that during 04:00–05:00 UTC on January 15, 2022, five explosions took place, with the most powerful at about 04:15 UTC, which was associated with an earthquake of Richter magnitude 5.8.

It is generally accepted that the energy of a volcanic explosion is the key parameter for atmospheric stability during the period of an active explosion. It establishes the magnitude of disturbances in the atmosphere, ionosphere, and magnetosphere, which are indirectly responsible for the generation of waves due to the mechanical pressure change in the ambient atmosphere or seismic shaking of the ground and propagate vertically through different layers in combination with the earth's gravitational field. The mechanisms of coupling between different atmospheric layers during this type of explosion could be different, like seismo-electromagnetic mixing

of chemical and physical processes proposed by Pulinets and Ouzounov (2018) and wave-induced vertical coupling between the lower and upper atmospheres, which transfer momentum and energy from lower levels to much higher altitudes during volcano eruptions (Dautermann *et al.* 2009) and earthquakes (Zhang *et al.*, 2023). In another event in 1991, after the Mt. Pinatubo eruption, an evident increase in gravity wave activity at long periods (T > 120 min) was revealed, which was a very good coincidence with the large increase in the volcanic aerosol optical depth (Lastovika, 2003; Khaykin *et al.,* 2022). Generally, gravity waves and their changes with altitude in the middle atmosphere are significantly affected by the background wind and temperature fields, which affect the propagation and dissipation of gravity waves (Kazimirovsky, 2002; Lastovicka, 2006; Vincent, 2007). But it's debated if it could happen before an eruption or earthquake. In this study, an attempt has been made to address this important point, especially before an eruption and/or explosion.

So far, almost all studies have used ground-based information (Rozhnoi *et al.,* 2014), HF (high-frequency) Doppler radar, VLF, and GNSS (Dautermann *et al.,* 2009; Sellitto *et al.*, 2022; Themens *et al.*, 2022) to study the impact of an explosion or eruption on the atmosphere-ionosphere system. In this study, COSMIC satellite data have been used to study the ionospheric variation during the pre-eruption, eruption, and post-eruption periods of the HTHH volcano explosion. A span of 62 days of observational period (i.e., 1st December-21 to 31st January-22) has been considered, which includes two major events of explosion: one across 20-21st December-2021 and another on January 15, 2022. The central point of the present paper is to analyze the diurnal variations of ionospheric peak parameters (NmF2 and HmF2) in the F2 layer, bottom-side integrated electron content (BIEC), and top-side integrated electron content (TIEC) during the observational period.

MATERIAL AND METHOD OF ANALYSIS

For any observational study, data acquisition is one of the most important criteria for carrying it out properly. Here, the space-based observation has been considered to acquire information about the ionosphere, and finally, COSMIC satellite data (namely "ionPrf" data on the COSMIC satellite website, a level 2 vertical profile data) has been taken from its website at (http://www.cosmic.ucar.edu) for the 62-day observational period (i.e., 1st December 21 to 31st January 22). To examine the solar activity, solar flux data at 10.7 cm (F10.7) has been taken from the World Data Centre (WDC) website at http://www.ukssdc.ac.uk, and the $\sum \mathrm{Kp}$ index information has been taken from the Kyoto University website ("WDC,n.d.) at http://wdc.kugi.kyoto-u.ac.jp to analyse geomagnetic activity for the entire observation period (1st December 21 to 31st January 22).

Technically, COSMIC satellites take nearly 100 minutes to complete one round of earth (Adhikari *et al.,* 2021) and to have ionospheric information at a particular moment for a fixed place is rarely possible. To overcome this challenge, a $15^{o} \times 15^{o}$ boxcar region cantered at the point of location (HTHH) was considered to accumulate the maximum number of vertical electron density (VED) profiles. As the first step of the filtration technique, those profiles were shorted out, in which the geographic latitude (GEO_LAT in the VED profile) and geographic longitude (GEO_LON in the VED profile) of HmF2 lie within 12S-27S and 3E-168W. Finally, those VED profiles have been taken into consideration for analysis, which were associated with $F10.7 \leq 150$ sfu, and $\sum Kp \leq 30$. All the VED profiles considered here are in NETCDF format, and the information about ionospheric peak parameters (i.e., NmF2 and HmF2) can easily be extracted from them. Remaining two parameters, BIEC (IEC is equivalent to TEC and 1TECU=1E+16 el/m^2) and TIEC were calculated using the equations: (1)

$$(BIEC, TIEC) = \int_{(Balt, HmF2)}^{(HmF2, Talt)} Ne(z)dz \qquad (1)$$

In the above equation (Eq. 1), Balt and Talt are the Mean Sea Level Altitude (MSL_Alt) at the bottom and top point of the bottom and topside Ionosphere respectively. To curtail the effect of diurnal variability in the

ionospheric signature to be detected, if any, we finally calculate the daily weighted mean of each parameter using equation (2). Each day (i.e., 24 hours) is being divided into four equal-length (six hours) LT sub-intervals: $0 \leq LT < 6$, $6 \leq LT < 12$, $12 \leq LT < 18$, and $18 \leq LT < 24$, and thereafter, all the parameters associated with these four sub-intervals have been assigned the weights 4, 3, 2, and 1, respectively

$$P(\text{ave}) = \frac{(4N_4P + 3N_3P + 2N_2P + N_1P)}{(4N_4 + 3N_3 + 2N_2 + N_1)} \quad (2)$$

Now the Electron Content Ratio (ECR) (Mondal *et al.*, 2014) calculated using equation (3)

$$ECR = TIEC / BIEC \quad (3)$$

Another parameter the Semi-thickness ratio (RTB) is calculated using the formula (Gulyaeva et al., 2007):$RTB = B0top/B0bot$ *(4)*

Where B0bot and B0top are the Bottom-side Semi-thickness (B0bot) and Topside Semi-thickness (B0top) parameters, calculated for the half-peak density (Ne=0.5*NmF2) height below and above the F2 peak (HmF2). Details description about ECR and RTB have been given in Mondal *et al.*, 2014, Gulyaeva, 2007

RESULT AND DISCUSSION

VARIATION IN NmF2 AND HmF2

Figure 2 shows the variability in peak electron concentration (NmF2) in the F2 layer with corresponding height levels of HmF2 for the 62-day observational period starting from December 1st, 2021, to January 31st, 2022, which includes the pre-eruption and post-eruption periods of the HTHH volcano. Here, the daily weighted average values of NmF2 (see figure 2(a)) and HmF2 (see figure 2(b)) were plotted. Clearly, across the 12th of December 2021, a perturbation in the dense F2 layer triggered and ran till the 21st of December 2021, achieving peak value, while both NmF2 and HmF2 steadily increased day by day and thereafter maintained a certain level of higher value for the next 2-3 days at the height level (340–345 km), which is almost 15–17% higher than the normal level (~290–300 km). Then both parameters started decreasing from the top level, achieving normal, to below-normal values across January 5–6, 2022. (see Figure2).

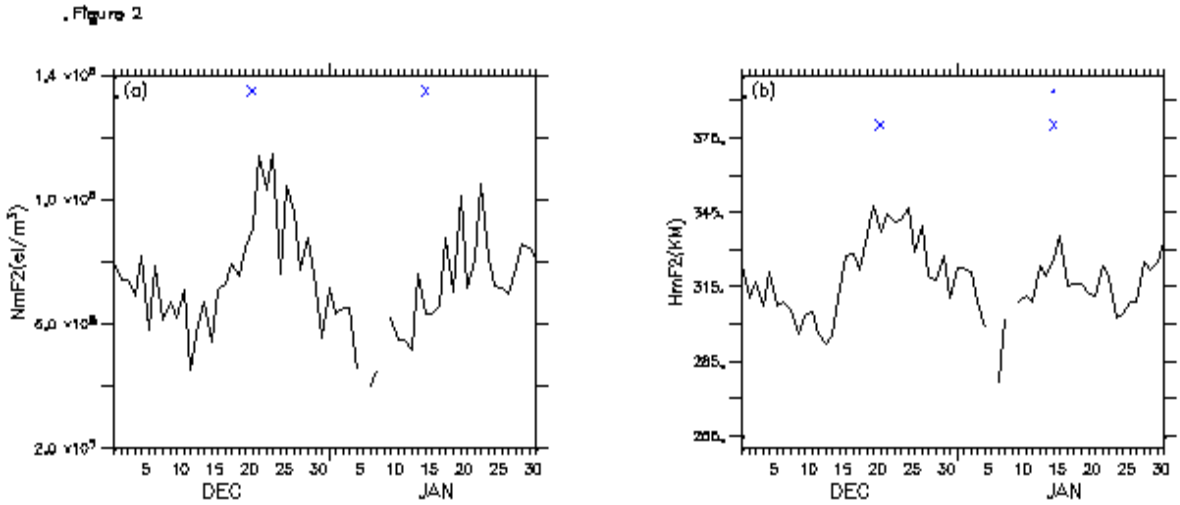

Fig. 2: Variation in peak ionospheric parameters (NmF2 and HmF2) during the 62 days observational period. Stars in each panel denote the days of occurrence of volcanic explosion.

Interestingly, again, a phase of apparent ascending NmF2 concentration with higher-high HmF2 starting from January 7th to January 17th, 2022, indicates another perturbation in the dense ionosphere, specifically in the topside dense F2 region, which might be correlated to disturbances in the lower atmosphere due to the combined effect of earthquakes of a wide spectrum of magnitude (Matoza *et al.,* 2022) and changes in atmospheric constituents during the preparation stage of a large volcanic explosion as well as during the active eruption period of the HTHH volcano, partly consistent with the result of Miyoshi and Shinagawa, 2023. So, giving insight into the variation of NmF2 and HmF2, it might be noted that the ionosphere shows a clear signature during pre-eruption as well as during the active eruption stage of any volcano.

VARIATION IN TECs (i.e. TTEC and BTEC)

In figure 3, TEC values were plotted for the 62-day observational period starting from December 1, 2021 to January 31, 2022. As it is well established that TEC (total electron content) is the proxy of electron distribution throughout the ionosphere in the vertical direction, two panels in figure 3 exhibit a sensitive variation in Ne concentration corresponding to the bottom and top sides of the ionosphere. In this figure, we can clearly identify two cycles in TEC concentration in the entire observation period, though the solar activity and geomagnetic activity in the entire observation period were quite normal. In the first cycle, both TECs started to increase from the 13th of December 2021, achieving a peak across the 23rd of December 2021, which could be treated as the rising phase of the first cycle. In this case, both TECs increased by about 3.5–3.8 times with respect to their normal level on December 13. Thereafter, a drastic descending phase was observed in both TECs with comparatively high fluctuation until January 5, 2022, and achieved a level almost equivalent to the previous low. But, after a short period of time, this descending phase paused, and suddenly another ascending phase started just after January 5–6, 2022, which is termed the second cycle of variability in TEC concentration in both the bottom and topside parts of the ionosphere. This ascending phase continued until January 18–20, 2022.

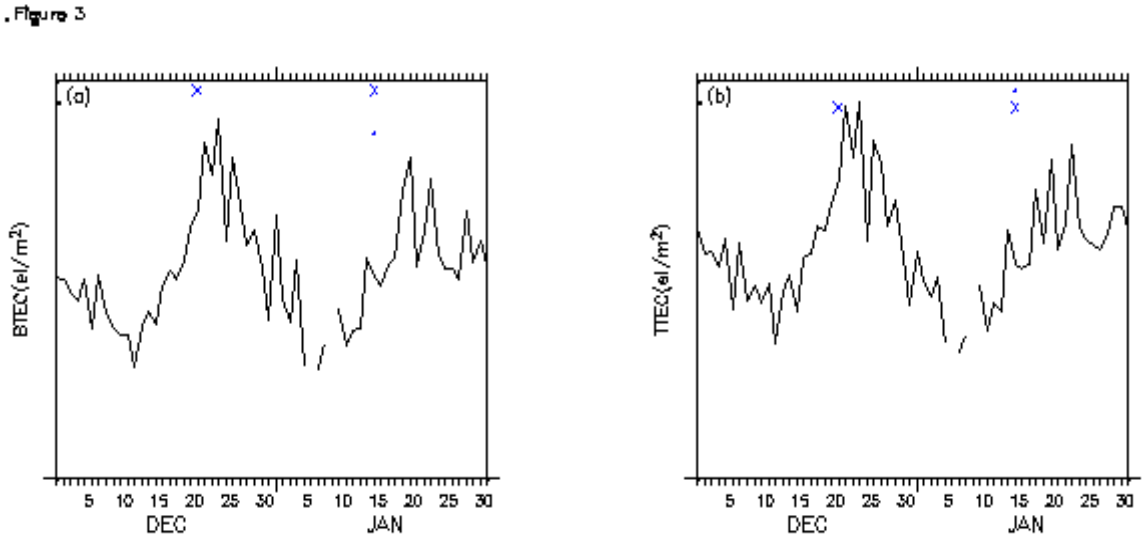

Fig. 3: Variation in ionospheric TECs (TTEC and BTEC) during the 62 days observational period. Stars in each panel denote the days of occurrence of volcanic explosion.

Though there were two major explosions in HTHH during this observation period, the last one on January 15, 2022, had a massive impact on the climate. Here, two distinct phases of variability in ionospheric parameters in the F2 region clearly exhibit the so-called coupling between the lower atmosphere and the ionosphere. Though the mechanism of this coupling may not be the same for different types of events, even at different stages of an event, in this case, a clear and steady increase in TECs during the pre-eruptive stage of the volcano, both in the bottom and topside parts of the ionosphere, significantly indicates that more and more charged particles were

accumulating during this phase. In the post-volcanic explosion phase, though different parameters in the lower atmosphere take time to achieve normalcy (Jenkins *et al.*, 2023; Taha *et al.*, 2022), the ionosphere attains the normal stage comparatively faster.

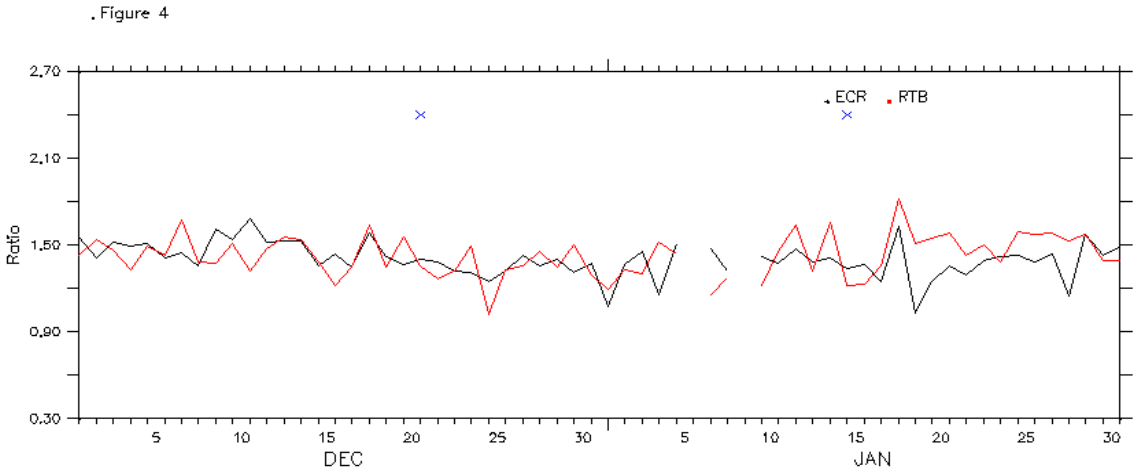

Fig. 4: Variation in ECR (Electron Content Ratio) and RTB (Semi-Thickness Ratio) during the 62 days observational period. Stars denote the days of occurrence of volcanic explosion.

HmF2 (see figure 2(b)) gradually increasing means more and more Ne concentration in the dense plasma region of the topside F2 layer, resulting in BTEC and TTEC increasing. Actually, BTEC is dominating in the pre-eruption period as the highest range of the bottom side ionosphere is increasing while that of the topside ionosphere is decreasing. Hence, ECR and RTB (see figure 4) get lower values during the pre-eruption phase, whereas in the post-eruption phase, as HmF2 (see figure 2(b)) decreases and NmF2 (see figure 2(a)) gets lower levels of concentration, this ratio is increasing.

VARIATION IN E LAYER

Figure 5 depicts the distribution of electrons (Ne) in the E layer during the observational period covering the HTHH volcanic eruption. In this case too, two specific cycles of Ne concentration were observed in the total observational period. Up to December 24th, 2021, both peak electron concentration level and total electron content in the E layer (ETEC) fluctuate within a stable range from their mean with normal to below normal level concentration, while the 1st explosion in the HTHH volcano happens across December 20th–21st, 2021. After that, in the post-explosion/eruption phase, a sharp increase in electron (Ne) concentration throughout the E layer (both Ne and ETEC) was detected, which exhibits a perturbation in this region due to some external forcing persisting for the next 2–3 days. After December 27, 2021, electron concentration throughout the E layer decisively decreased from the higher level to achieve previous normalcy and afterward maintained a steady level for the next few days. Similarly, in the second cycle, during the preparation phase (up to January 15th, 2022) to the active explosion phase, Ne concentration was either normal or below normal, whereas in the post-explosion phase, Ne concentration exhibits a noticeable increase with high fluctuations.

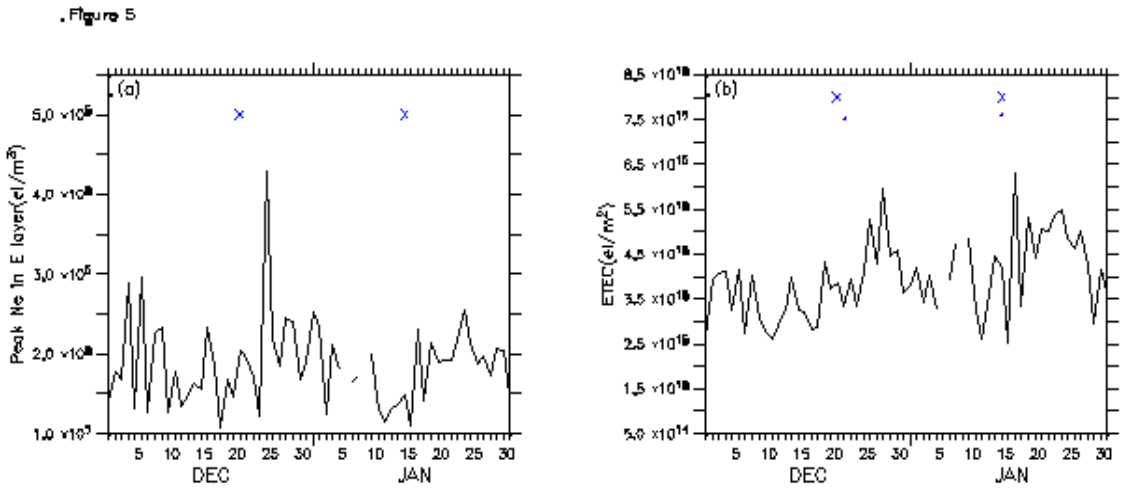

Fig. 5: Variation in E-layer electron concentration and ETEC during the 62 days observational period. Stars denote the days of occurrence of volcanic explosion.

If we concentrate on the lower atmosphere, during this period a plume was formed with the help of a huge amount of ejected pyroclastic material due to the volcanic eruption in the lowermost part of the atmosphere, and gradually its height was increasing up to ~58 km, creating an umbrella cloud with a radius of ~500 km (Chernogor, 2022; Taha *et al.,* 2022). The energy released during this volcanic eruption is mostly in the form of thermal energy from eruptive materials, which triggers a number of waves of different physical nature, like seismic waves, tsunami waves, blast waves, lamb waves, atmospheric gravity waves, infrasound, and sound waves (Wright *et al.,* 2022). Some of these types of waves are manifestations of coupling between different layers of the Earth-Atmosphere-Ionosphere system during their different phases of life cycle (Kazimirovsky, 2002; Lastovicka, 2006; Vincent, 2007; Chernogor, 2022).

CONCLUSIONS

Five major findings in this study are as follows:

1. Two cycles of variability in HmF2, NmF2, BTEC, and TTEC clearly indicate the coupling between the ionosphere and lower atmospheric disturbances associated with two volcanic explosions.
2. Two cycles were associated with two explosions and/or eruptions. In each cycle, raising phases were associated with the preparation phase of the explosion and/or eruption, whereas falling from the top towards the normal level to below the normal level was associated with the post-eruptive phase of the volcano.
3. For the E layer, the peak Ne concentration and ETEC both showed normal to below-normal concentrations in the pre-explosion/eruption phase, whereas a sharp increase occurred during the post-explosion, mostly in agreement with the report of Lastovika 2003.
4. In the dense ionosphere (i.e., in the F layer), the pre-explosion/eruption signature is more prevalent than in the lower ionosphere, i.e., the E layer, which is one of the major findings of this study.

However, in-depth studies related to the mechanism of this coupling between volcanic eruptions and the ionosphere need to be explored in more cases.

ACKNOWLEDGMENTS

COSMIC satellite data were downloaded from the website http://www.cosmic.ucar.edu. Cyclone-related information has been taken from the IMD website http://www.imd.gov.in/. The author would like to thank WDC Geomagnetic Data Centre, Kyoto University, Japan for providing geomagnetic indices and UKSSDC, UK for

providing F10.7 cm solar flux data. The author would also like to acknowledge the reviewers for their earnest comments.

REFERENCES

Adhikari, L., Ho, S. P., and Zhou, X., 2021. Inverting COSMIC-2 Phase Data to Bending Angle and Refractivity Profiles Using the Full Spectrum Inversion Method, *Remote Sens.* 2021, *13*(9), 1793; https://doi.org/10.3390/rs13091793

Besl, J. 2023. Tonga eruption may temporarily push Earth closer to 1.5°C of warming, *Eos, 104,* https://doi.org/10.1029/2023EO230104.

Carn, S. A., Krotkov, N. A., Fisher, B. L. and Li, C. 2022. Out of the blue: Volcanic SO2 emissions during the 2021–2022 eruptions of Hunga Tonga—Hunga Ha'apai (Tonga). Front. Earth Sci. 10:976962. doi: 10.3389/feart.2022.976962

Chernogor L. F. V. N. 2022. Physical effects from the powerful Tonga volcanic eruption of January 15, 2022, in the Earth–atmosphere–ionosphere–magnetosphere system, Karazin Kharkiv National University, 4 Svobody Sq., Kharkiv, 61022 Ukraine

e-mail: Leonid.F.Chernogor@gmail.com

Dautermann, T., Calais, E., Lognonné, P., and Mattioli, G.S. 2009. Lithosphere–Atmosphere–Ionosphere Coupling after the 2003 Explosive Eruption of the Soufriere Hills Volcano, Montserrat. Geophys. J. Int. 179, 1537–1546

Gulyaeva, T. L., 2007. Variable coupling between the bottomside and topside thickness of the ionosphere, Journal of Atmospheric and Solar-Terrestrial Physics, 69, 4–5, 528-536, https://doi.org/10.1016/j.jastp.2006.10.015

Heidarzadeh, M., Gusman, A. R., Ishibe, T., Sabeti, R., and ˇSepi´e, J., 2022. Estimating the eruption-induced water displacement source of the 15 January 2022 Tonga volcanic tsunami from tsunami spectra and numerical modelling, Ocean Engineering,

https://doi.org/10.1016/j.oceaneng.2022.112165

JENKINS, S., SMITH, C., ALLEN, M., & GRAINGER, R., 2023. TONGA ERUPTION INCREASES CHANCE OF TEMPORARY SURFACE TEMPERATURE ANOMALY ABOVE 1.5 °C, NATURE CLIMATE CHANGE , 13, 127–129

Kazimirovsky, E. S., 2002. Coupling from below as a source of ionospheric variability: a review. Ann. Geophys. 45(1), 1-29

Khaykin, S., Podglajen, A., Ploeger, F., Groo, J. U., Tence, F., Bekki S., Khlopenkov K., Bedka, K., Rieger, L., Baron, A., Beekmann, S. G., Legras, B., Sellitto, P., Sakai T., Barnes, J., Uchino, O., Morino, I., Nagai, T., Wing, R., Baumgarten, G., Gerding, M., Duflot, V., Payen, G., Jumelet, J., Querel, R., Liley, B., Bourassa, A., Clouser, B., Feofilov, A., Hauchecorne, A., & Ravetta F., 2022. Global perturbation of stratospheric water and aerosol burden by Hunga eruption, 3, 316, *Communications Earth & Environment*, https://www.nature.com/articles/s43247-022-00652-x.

Lastovika, J., 2003, Impact of the Mt. Pinatubo volcanic eruption on the lower ionosphere and atmospheric waves over Central Europe, ANNALS OF GEOPHYSICS, 46, 6.

Lastovicka, J., 2006. Forcing of the ionosphere by waves from below. J. Atmos. Sol.-Terr. Phys. 68, 479–497, http://doi.org/10.1016/j.jastp.2005.01.018.

Miyoshi, Y., and Shinagawa, H., 2023. Upward propagation of gravity waves and ionospheric perturbations triggered by the 2022 Hunga-Tonga volcanic eruption, *Earth, Planets and Space (2023) 75:68* https://doi.org/10.1186/s40623-023-01827-2

Mondal, G., Gupta, M., Sen, G. K., 2014. Variation in electron Content Ratio and Semi-thickness Ratio during LSA and MSA periods and some Cyclone Genesis Periods using COSMIC satellite observations; Advances in Space Research 54 2151-2158.

Pulinets, S., Ouzounov, D., Karelin, A., and Davidenko, D., 2018. Lithosphere-Atmosphere-Ionosphere-Magnetosphere Coupling-A Concept for Pre-Earthquake Signals Generation. In Pre-Earthquake Processes: A Multidisciplinary Approach to Earthquake Prediction Studies; Ouzounov, D., Pulinets, S., Hattori, K., Taylor, P., Eds.; Geophysical Monograph Series; John Wiley & Sons, Inc.: Hoboken, NJ, USA, 2018; 77–98. ISBN 978-1-119-15694-9

Ragone, A. H. C. D., Manzano, A. N. F. D., Elias, A. G., and Artigas, M. Z. D, 2004. Ionospheric effects of volcanic eruptions, Geofísica Internacional, 43, 2,187-192 .

Schoeberl, M. R., Wang, Y., Ueyama, R., Taha, G., Jensen, E., & Yu, W., 2022. Analysis and impact of the Hunga Tonga-Hunga Ha'apai stratospheric water vapor plume. *Geophysical Research Letters*, *49*, e2022GL100248. https://doi.org/10.1029/2022GL100248

Sellitto, P., Podglajen, A., Belhadji, R., Boichu, M., Carboni, E., Cuesta, J., Duchamp, C., Kloss, C., Siddans, R., Bègue, N., Blarel, L., Jegou, F., Khaykin, S., Renard, J. B. & Legras, B., 2022. The unexpected radiative impact of the Hunga Tonga eruption of 15th January 2022, COMMUNICATIONS EARTH & ENVIRONMENT, 3:288, https://doi.org/10.1038/s43247-022-00618-z;

Shinbori, A., Otsuka, Y., Sori, T., Nishioka, M., Perwitasari, S, Tsuda T., and Nishitani, N., 2022. Electromagnetic conjugacy of ionospheric disturbances after the 2022 Hunga Tonga-Hunga Ha'apai volcanic eruption as seen in GNSS-TEC and Super DARN Hokkaido pair of radars observations, *Earth, Planets and Space 74:106,* https://doi.org/10.1186/s40623-022-01665-8

Taha, G., Loughman, R., Colarco, P. R.,Zhu, T., Thomason, L. W., & Jaross,G. 2022. Tracking the 2022 HungaTonga-Hunga Ha'apai aerosol cloud in the upper and middle stratosphere using space-based observations. *Geophysical Research Letters*, *49*, e2022GL100091.https://doi.org/10.1029/2022GL100091

Themens, D. R., Watson, C., Žagar, N., Vasylkevych, S., Elvidge, S., McCaffrey, A., 2022. Global propagation of ionospheric disturbances associated with the 2022 Tonga volcanic eruption. Geophysical Research Letters, 49, e2022GL098158. https://doi.org/10.1029/2022GL098158

Vincent, R. A., 2007. Gravity wave coupling from below: A review. Climate and Weather of the Sun-Earth System (CAWSES), Kyoto Symposium, 279–293, https://www.terrapub.co.jp/onlineproceedings/ste/CAWSES2007/pdf/CAWSES_279.pdf.

Wright, C. J., Hindley, N. P., Alexander, M, J., Barlow, M., Hoffmann, L., Cathryn N. Mitchell, C. N., Prata, F., Bouillon, M., Carstens, J., Clerbaux, C., Osprey S. M., Powell, N., Randall C., E, & Jia Yue. J., 2022. Surface-to-space atmospheric waves from Hunga Tonga–Hunga Ha'apai eruption, Nature, 609, 741-746, https://doi.org/10.1038/s41586-022-05012-5

Zhang H., Zhu, K., Cheng, Y., Marchetti, D., Chen, W., Fan, M., Wang, S., Wang, T., Zhang, D., Zhang, Y., 2023. Atmospheric and ionospheric effects of La Palma volcano 2021 eruption, doi: 10.20944/preprints202307. 0245.v